Docking, synthesis and *in vitro* evaluation of antimitotic estrone analogs

Authors: B.A. Stander[a], F. Joubert[b] and A.M. Joubert[a]

[a] *Department of Physiology, University of Pretoria, P.O. Box 2034, Pretoria 0001, South Africa*

[b] *Bioinformatics and Computational Biology Unit, University of Pretoria, 0002 Pretoria, South Africa*

Abstract

In the present study, Autodock 4.0 was employed to discover potential carbonic anhydrase IX inhibitors that are able to interfere with microtubule dynamics by binding to the Colchicine binding site of tubulin. Modifications at position 2' of estrone were made to include moieties that are known to improve the antimitotic activity of estradiol analogs. 2-ethyl-3-*O*-sulphamoyl-estra-1,3,5(10),15-tetraen-3-ol-17-one estronem (C9) and 2-ethyl-3-*O*-sulphamoyl-estra-1,3,5(10)16-tetraene (C12) were synthesized and tested *in vitro*. Growth studies were conducted utilizing spectrophotometrical analysis with crystal violet as DNA stain. Compounds C9 and C12 were cytotoxic in MCF-7 and MDA-MB-231 tumorigenic and metastatic breast cancer cells, SNO non-keratinizing squamous epithelium cancer cells and HeLa cells after 48 h exposure. Compounds C9 inhibited cell proliferation to 50% of the vehicle-treated controls from 110-160 nM and C12 at concentrations ranging from 180-220 nM. Confocal microscopy revealed abnormal spindle morphology in mitotic cells. Cell cycle analysis showed an increase in the number of cells in the G_2/M fraction after 24 h and an increase in the number of cell in the sub-G_1 fraction after 48 h, indicating that the compounds are antimitotic and able to induce apoptosis.

Introduction

Most of the chemotherapeutic anti-cancer drugs used in the clinic today include agents that target the cell cycle in order to inhibit hyperproliferation of cancer cells and subsequently to induce apoptosis (1-3). Microtubule-interfering drugs bind to microtubules at diverse sites. Vinblistine binds at the plus end and inhibits microtubule polymerization (4). Colchicine forms complexes between the α- and β-tubulin dimers to suppress microtubule dynamics and paclitaxel binds along the interior surface of the microtubule, thereby interfering with the dynamics of microtubules (4). Various agents that bind to the colchicine binding site of microtubules are in various stages of clinical trials. These include combretastatins and its analogs as well as 2-methoxyestradiol (2ME) (5-6).

2-Methoxyestradiol (2ME) is an endogenous metabolite of 17*β*-estradiol exerting both antiangiogenic and antimitogenic effects *in vitro* and *in vivo* (7). Abrogation of microtubule dynamics is one of the mechanisms of action of 2ME and it is proposed that 2ME interacts with the colchicine binding site of

microtubules (5, 8). 2ME has short half life and has been shown to be a target for 17β-hydroxysteroid dehydrogenase-mediated metabolism (9). It is thus important to develop novel 2ME derivatives that are able to improve bioavailability and potency.

Sulphamates, including sulphamoylated derivatives of 2ME, have increased bioavailability because they are able to transit the liver without undergoing first pass metabolism (10-12). This is due to the ability of sulphamoylated derivatives to reversibly bind to carbonic anhydrase II (CAII) in red blood cells after which they are then slowly released into the blood circulatory system (10). Carbonic anhydrases are zinc enzymes that catalyze the conversion of carbon dioxide and water to carbonic acid (13). Tumor cells have a lower extracellular pH than normal cells and the acidotic environment promotes the action of growth factors and proteases involved in tumor progression (14). CAIX is overexpressed in a variety of tumors and is implicated in the acidification of the extracellular environment of tumors (15-16). The CAIX gene contains a hypoxia-response element (HRE) that binds active HIF-1α and induces the transcription of CAIX (15). The characteristic hypoxic microenvironment of tumors together with the HRE of the CAIX gene explains the overexpression of CAIX in a variety of tumors (15). Selective inhibition of CAIX provides a valuable strategy for curtailing the development of metastatic processes associated with acidotic microenvironmental conditions in tumors. The aim of this study was to identify potential carbonic anhydrase IX inhibitors that are capable of interfering with microtubule dynamics.

Materials and Methods

Materials

Heat-inactivated fetal calf serum (FCS), sterile cell culture flasks and plates were obtained through Sterilab Services (Kempton Park, Johannesburg, South Africa). Dulbecco's minimum essential medium Eagle (D-MEM), penicillin, streptomycin and fungizone were purchased from Highveld Biological (Pty) Ltd. (Sandringham, SA). A primary anti-tubulin alpha antibody from IMGENE (Alexandria, Virginia, USA) (cat no. IMG-80196) was purchased from BIOCOM biotech (Pty) Ltd. (Clubview, South Africa). The Alexa Fluor® 488, anti-mouse IgG H+L secondary antibody from Invitrogen (Carlsbad, California, USA) (cat no. A21202) was purchased from The Scientific Group (Johannesburg, South Africa). All other chemicals were of analytical grade and were purchased from Sigma Chemical Co. (St. Louis, MO, USA).

Software

The Chimera package from the Resource for Biocomputing, Visualization, and Informatics at the University of California, San Francisco (supported by NIH P41 RR-01081) was used for structure preparation and visualization (17). Reduce was used for adding hydrogens to the receptor PDB molecular structure files (18). Ligand conformational searches for X-ray ligands were performed with VEGA 2.2.0

(19). Docking studies were carried out with Autodock 4.0 and AutoDockTools4 (Scripps Research Institute, La Jolla, CA, USA) (20). AutoDock4 evaluates the energies for both the bound and unbound states and uses a semiempirical free energy force field by taking into account hydrogen bonding, electrostatic interactions, deviation from covalent geometry, internal ligand torsional constraints, and desolvation effects (20). On average, a standard error of about 2–3 kcal/mol in prediction of binding free energy in cross-validation studies was found and this was found to be good enough to differentiate between nM, μM and mM activity of leads (20). ACD/ChemSketch was used to generate Simplified Molecular Input Line Entry System (SMILES) annotations of ligands (21). 3-Dimensional (3D) PDB atomic coordinates were generated from the SMILES annotations by the Online SMILES Translator[a] service provided by the Computer-Aided Drug Design (CADD) Group and the National Cancer Institute (NCI). Protein structures for docking were gathered from the Research Collaboratory for Structural Bioinformatics (RCSB) Protein Data Bank.

Docking methodology

Human CA II, is one of the most commonly studied enzymes with 279 X-ray crystallographic structures and a wealth of information regarding various inhibitors of CAII (22). Tuccinardi *et al.* (2007) determined via cross-docking analysis using the ChemScore GOLD docking program that the 1OKN, 1KWR, 1CIM, 1BNW, 1CNX, 1OQ5 and 1TTM X-ray structures displayed the best RMSD average of the redocked ligands (23). These receptors were chosen to be employed in the present study as part of an ensemble docking study (24). Ligands extracted from 52 human CAII X-ray structures (Supporting Information S1) were redocked into the selected receptors and the best score of each ligand was chosen. The correlation between the calculated Autodock 4.0 free energy of binding ($AD4_{\epsilon}$) and the experimentally determined inhibition constant ($expK_i$) as well as the root mean squared deviation (RMSD) of the docked ligand compared to the X-ray structure were calculated. Genis *et al.* (2009) developed an effective mimic of CAIX for use in high-throughput screening of potential CAIX inhibitors (25). The structures (3DC9, 3DCS, 3DCC, 3DC3, 3DCW and 3DBU) generated from the study were included in the docking study. 5 structures of tubulin were available (1SA0, 1SA1, 1Z2B, 3DU7, and 3E22) with two Colchicine binding sites each. Both were used for the ensemble docking to give a final total of 10 tubulin receptors. The Lamarckian genetic algorithm for conformational searching was used in Autodock with the ga_pop_size and ga_num_evals parameters set to 250 and 2500000 respectively.

Receptor preparation

For receptor preparation, ligands, waters and other HET groups where removed. The water molecule between ASN62, ASN67 and GLN92 in the carbonic anhydrase receptors were included in docking

simulations because they are present in most of the X-ray proteins analyzed (23). Hydrogens were added by making use of the Reduce software. The software adds in a standardized geometry with optimization of the orientations of OH, SH, NH_3^+, Met methyls, Asn and Gln sidechain amides, and His rings (18). After adding hydrogens, the Assisted Model Building with Energy Refinement (*AMBER*) Antechamber module (included with Chimera) was used to assign the Generalized *AMBER* force field (GAFF) types and atomic partial charges to each atomic residue of the PDB structure (26-27). After addition of hydrogens and atomic partial charges, the receptors were minimized utilizing the Amber ff99ua forcefield as implemented in Chimera (27-28). 1000 steps (step size of 0.02 Angstrom) of constrained minimization of the hydrogen network was followed by 500 steps (step size of 0.02 Angstrom) of side chain atoms to allow for internal hydrogen bond formation and removal of any internal clashes. After minimization, the respective tubulin, CAII and CAIX proteins were superimposed by the MatchMaker module in Chimera. The AD4_bound.dat parameters of Autodock 4.0 were used for receptor preparation and docking. Receptors were prepared with the prepare_receptor4.py script by adding Gasteiger charges and merging non-polar hydrogens. The zinc ion charge of carbonic anhydrase receptors was set to +2.

Ligand Preparation

The ligands of 52 CAII-inhibitor complex structures from the RCSB) Protein Data Bank were extracted (Supporting Information S1). In order to generate a library of modified estradiol ligands, several modifications were made at positions 2 and the D-ring in order to generate a library of leads with potential antimitotic and anti-carbonic anhydrase activity (Supporting Information S2). Position 3 was replaced with a sulphamate group. Modifications at position 2 were made to include moieties that are known to improve the antimitotic activity of estradiol analogs. Cushman *et al.* (1995) demonstrated that 2-((*E*)-1'-propenyl and 2-ethoxy and substitutions improve the antimitotic activity of estradiol on several cancer cell lines (29). Leese *et al.* (2004) demonstrated that a 2-methylsulphanyl substitution of estradiol greatly enhanced anti-proliferative activity while the 2-ethyl substitution enhanced anti-mitotic activity even more (11, 30). Therefore, 2-methoxy, 2-ethoxy, 2-ethyl, 2-methylsulphanyl and 2-((*E*)-1'-propenyl derivatives were included in the lead library (Supporting Information S1). D-ring modifications that are known to improve the anti-proliferative activity of estradiol analogues were also included. These include the 17-1'-methylene substitution discovered by Edsall *et al*. (2004) (31). Dehydration at positions 14 and 15 was shown to have increased anti-proliferative and anti-tumour activities (32). The 16-dehydrated anti-mitotic analogue of 2ME (ENMD-1198) also shows promise and is currently undergoing clinical trials, therefore dehydration at position together with double dehydration at position 14 and 16 were included in the library of lead ligands (33-34). 17-*O*-sulphamate as well as 17-deoxy-17-cyano substitutions have also shown promise and were thus included in the docking study (35). 17-hydroxy as well as 17-keto substitutions were also considered. All the modifications were made to generate a library of leads containing 85 ligands (Supporting Information S1).

Hydrogens were added to all ligands with VEGA. The ligands were subjected to a conformational search of 1000 steps in VEGA (19). The systematic method with the SP4 forcefield and AMMP-MOM charges were used for the conformational search and minimization (20 steps, Toler = 0.01). Finally, the ligands were prepared for docking with AutoDockTools4 with the prepare_ligand4.py script. The charge of the zinc-binding nitrogen was changed to 0.800 (0.800 NA) and the charge of the hydrogen of the zinc-binding nitrogen was changed to -0.300 (-0.300 HD). This change improved docking conformations by constraining docking simulations to correctly form bonds between the sulfonamido nitrogen of the ligand and the zinc ion, as well as the hydrogen bond between the sulfonamido nitrogen's hydrogen and Thr199 in the docked conformations.

Chemistry

The synthesis of lead compounds was outsourced to iThemba Pharmaceuticals (Pty) Ltd (Modderfontein, Gauteng, South Africa). All chemicals were purchased from Aldrich Chemical Co (St. Louis, MO, USA). Organic solvents of A.R. grade were used as supplied. Anhydrous *N,N*-dimethylformamide and *N,N*-dimethylacetamide were purchased from Aldrich and stored under a positive pressure of N_2 after use. Tetrahydrofuran was distilled from sodium. Sulphamoyl chloride was prepared by an adaptation of the method of Appel and Berger and stored in a tightly sealed container in the fridge (36). Chromatography was performed on silica gel (70–230 mesh, Macherey Nagel). Thin layer chromatography was performed on Alugram® SIL G/UV_{254} aluminium backed plates (Macherey Nagel). Products were visualized with basic potassium permanganate solution. ^{1}H NMR spectra were recorded in deuterated chloroform solution (unless otherwise indicated) with a Varian 400 NMR spectrometer at 400 MHz. Chemical shifts are reported in parts per million (ppm, δ) relative to tetramethylsilane (TMS) as an internal standard. Compounds were synthesized according to scheme 1 in Figure 1 and Supporting Information S1. All the compounds were >90% pure and were analyzed by high resolution mass spectrometry (HR-MS) (Wits University, Johannesburg, South Africa), and NMR as described in Supporting Information S3 and S4.

Cell culture

MCF-7 (estrogen receptor positive) breast cancer cells, MDA-MB-231 (estrogen receptor negative) tumorigenic and metastatic breast cancer cells, SNO non-keratinizing squamous epithelium cancer cells and HeLa (human epithelial cervix carcinoma) cells were cultured in Dulbecco's minimum essential medium Eagle (DMEM) and supplemented with 10% heat-inactivated FCS (56°C, 30 min), 100 U/ml penicillin G, 100 µg/ml streptomycin and fungizone (250 µg/l). The synthesized compounds were dissolved in dimethyl sulphoxide (DMSO) in different stock concentrations depending on the activity of each compound in order to allow the final concentration of DMSO not to reach levels greater than 0.05%

in cell culture. Experiments were conducted in either 96-well plates or 6-well plates. For six-well plates, exponentially growing cells were seeded at 250 000 cells per well in 3ml maintenance medium in 6-well plates on heat-sterilized coverslips. After a 24 h incubation period at 37°C to allow for cell adherence, cells were exposed to the compounds including the vehicle- control and incubated for 24 h at 37°C. For 96-well plates, exponentially growing cells were seeded at 5000 cells per well to a final volume of 200 µl of maintenance medium. After 24 h attachment the medium was discarded and the cells were exposed o the compounds including the vehicle- control and incubated for 48 h at 37°C.

Crystal violet assay for determination of antiproliferative activity

Quantification of fixated monolayer cells was spectrophotometrically determined employing crystal violet as a DNA stain. Staining cell nuclei of fixed cells with crystal violet allows for rapid, accurate and reproducible quantification of cell number in cultures grown in 96-well plates (37-38). Dose-dependent studies were carried out in order to determine the growth inhibitory effect on the various cell lines of the newly synthesized compounds. The growth inhibitory effect was calculated as described by the National Cancer Institute in order to compare the growth inhibition induced by the compounds on the various cell lines (39).

Confocal microscopy morphological observation of tubulin architecture

Confocal microscopy was employed to observe the effects of the new compounds on the cytoskeletal microtubule architecture of control and treated MDA-MB-231 cells. Cells were fixated with gluraraldehyde and alpha-tubulin will be immunostained with anti-alpha tubulin antibodies [b]. Anti-alpha tubulin antibodies were counter-stained with an Alexa-488 fluorescent probe and the nucleus was counter-stained with 4',6-diamidino-2-phenylindole (DAPI). Stained cells will be viewed with a Zeiss 510 META confocal laser microscope and figures were generated with Zeiss' ZEN 2009 software.

Flow cytometric analysis of cell cycle progression

Flow cytometry was employed to measure the DNA content of exposed and control cells in order to monitor the effect on cell cycle progression of MCF-12A, MCF-7 and MDA-MB-231 cells. Analysis was conducted by ethanol fixation and propidium iodide staining of cells. Propidium iodide was used to stain the nucleus in order to determine the amount of DNA present. Data from at least 10 000 cells was captures with CXP software (Beckman Coulter South Africa (Pty) Ltd) and analyzed with Cyflogic (CyFlo Ltd.). Time-dependent studies were conducted at intervals of 24 h and 48 h.

Results and Discussion

Docking results: Reference ligands docked into CAII

After docking the reference ligands of the CAII receptors, the $AD4_{\epsilon}=0.144\ln(\exp K_i)-9.809$ logarithmic function yielded a coefficient of determination (R^2) 0.5856 between $\exp K_i$ and $AD4_{\epsilon}$ (Figure 2). The RMSD values ranged from 0.42 to 3.67 (Figure 1 and Supporting Information S5). This result indicates that the docking software is able to at least differentiate between μM and nM active compounds.

Docking results: CAII vs CAIX

After docking the estrone analog ligands into the active sites of CAII and CAIX, it was observed that the 3-methoxy, 2-ethyl and 2-methylsulphanyl moieties performed better than the other sterically larger moieties in both isoforms of CAs (Supporting Information S6). 2-ethyl-3-O-sulphamoyl-estra-1,3,5(10)16-tetraene (Figure 1, compound 12), 2-ethyl-3-O-sulphamoyl-estra-1,3,5(10),15-tetraen-3-ol-17-one (Figure 1, compound 9) and 2-ethyl-17-(1'-methylene)estra-1,3,5(10)-trien-3-O-sulphamate (Supporting Information S2, test 50) had the best CAIX:CAII ratio of the compounds that have not been synthesized before (Supporting Information S6).

Docking results: Tubulin Colchicine binding site

After docking the ligands into the Colchicine binding site between the alpha and beta-dimers of the tubulin protein, it was revealed that the 2-ethyl derivatives performed better than all the other derivatives when compared to their corresponding D-ring modified analogs (Supporting Information S7). This is in agreement with the results of Leese *et al.* (2006) were it was discovered that an ethyl substitution at position 2' of estrone provided the optimal substituent for high antiproliferative activity (11). The docking software docked the 2-ethyl ligands in the hydrophobic pocket (ala180.A, ala250.B, leu242.B, leu248.B, leu252.B, leu255.B, lys352.B, and val318.B) of the Colchicine binding site of tubulin of the 3E22 structure. The sulfonamido nitrogen of the compounds is docked close to tyr202.B or the val238.B oxygen, allowing them to form possible hydrogen bonds (Figure 3). Based on the docking results of the analogs into the colchicine site and the CAIX:CAII ratio of the compounds, it was decided to synthesize the novel 2-ethyl-3-*O*-sulphamoyl-estra-1,3,5(10)16-tetraene and 2-ethyl-3-*O*-sulphamoyl-estra-1,3,5(10),15-tetraen-3-ol-17-one analogs. The 2-ethyl-17-(1'-methylene)estra-1,3,5(10)-trien-3-*O*-sulphamate estrone analog also performed well, however the synthesis of 2-ethyl-17-(1'-methylene)estra-1,3,5(10)-trien-3-O-sulphamate was not completed for the present project and remains a possibility for future projects.

Antiproliferative activity of the compounds using crystal violet DNA stain assay

The synthesized compounds were screened for antiproliferative activity using crystal violet as a DNA stain as described by Berry *et al.* (1996) (40). The assay was carried out on MCF-7 breast cancer cells (estrogen receptor positive) tumorigenic and metastatic MDA-MB-231 breast cancer cells, non-tumorigenic MCF-12A breast cells, SNO non-keratinizing squamous epithelium cancer cells and HeLa (human epithelial cervix carcinoma) cells. Compound 9 and 12 reduced cell proliferation in a dose-dependent manner in all tested cell lines. The GI_{50} concentrations for the compounds are summarized in Table 1. The GI_{50} concentration of each compound was used in the subsequent studies.

Confocal microscopy morphological observation of tubulin architecture

Confocal microscopy was employed to observe the effects of compounds 9 and 12 on the cytoskeletal microtubule architecture of control and treated MDA-MB-231 cells after 24 h exposure. MDA-MB-231 vehicle-treated control cells presented with normal nuclear morphology and tubulin architecture during interphase, prophase, metaphase, anaphase and telophase (Figure 4, Supporting Information S8 and S9). Compounds 9 and 12 showed a similar type of interference with the mitotic spindle with abnormal formation of mitotic spindles (Figures 5 and 6, Supporting Information S10 and S11). These results confirm that the newly synthesized compounds are antimitotic agents that interfere with the microtubule dynamics in actively dividing cells.

Flow cytometric analysis of cell cycle progression

DNA content of cells was measured as an indication of cells in the various stages of the cell cycle in order to determine the effect that compounds 9 and 12 have on cell cycle progression. An increase in the number of cells in the G_2/M fraction was observed in both compound 9- and 12-treated cells after 24 h when compared to the vehicle-treated control (Figure 7). Also, an increase in the sub-G_1 fraction was observed in both compound 9- and 12-treated cells after 24 h, indicating an increase in apoptotic activity (Figure 7). After 48 h, the majority of the cells treated with compounds 9 and 12 were in the sub-G_1 fraction (Figure 8). These results indicate that the compounds are able to induce G_2/M block after 24 h and the cells in the G_2/M block as a result of exposure to compounds 9 and 12 are more likely to enter apoptosis than remain in G_2/M arrest or re-enter the cell cycle.

Conclusion and Future Directions

In the present study, docking studies were performed to assess the binding modes of estrone derivatives into CAII, CAIX and the colchicine binding site of tubulin. Based on the computational analysis, the

compounds that performed the best in docking into the colchicine binding site and had the best CAIX:CAII ratio were synthesized. Two new compounds with antimitotic activity in the sub-μM range were synthesized. The compounds are able to interfere with microtubule dynamics, resulting in a mitotic block and causes subsequent induction of apoptosis. Future studies will focus on the binding mode of the compounds into the CAIX enzyme. With additional cellular-mechanistic studies, these compounds could lead to new candidates for the future development of antimitotic drugs that specifically target metastatic processes associated with acidotic microenvironmental conditions in tumors as a result of CAIX overexpression.

Notes

[a] http://cactus.nci.nih.gov/services/translate/

[b] http://www.olympusfluoview.com/applications/protocols/cellsandtissuestubulin.html

References

1. Schmidt M, Bastians H (2007) Mitotic drug targets and the development of novel anti-mitotic anticancer drugs. *Drug Resist Updat;*10: 162-81.

2. Mollinedo F, Gajate C (2003) Microtubules, microtubule-interfering agents and apoptosis. *Apoptosis;*8: 413-50.

3. Zhou J, Giannakakou P (2005) Targeting microtubules for cancer chemotherapy. *Curr Med Chem Anticancer Agents;*5: 65-71.

4. Jordan MA, Wilson L (2004) Microtubules as a target for anticancer drugs. *Nat Rev Cancer;*4: 253-65.

5. Kamath K, Okouneva T, Larson G, Panda D, Wilson L, Jordan MA (2006) 2-Methoxyestradiol suppresses microtubule dynamics and arrests mitosis without depolymerizing microtubules. *Mol Cancer Ther;*5: 2225-33.

6. Cirla A, Mann J (2003) Combretastatins: from natural products to drug discovery. *Nat Prod Rep;*20: 558-64.

7. Mooberry SL (2003) Mechanism of action of 2-methoxyestradiol: new developments. *Drug Resist Updat;*6: 355-61.

8. D'Amato RJ, Lin CM, Flynn E, Folkman J, Hamel E (1994) 2-Methoxyestradiol, an endogenous mammalian metabolite, inhibits tubulin polymerization by interacting at the colchicine site. *Proc Natl Acad Sci U S A;*91: 3964-8.

9. Newman SP, Ireson CR, Tutill HJ, Day JM, Parsons MF, Leese MP, et al. (2006) The role of 17beta-hydroxysteroid dehydrogenases in modulating the activity of 2-methoxyestradiol in breast cancer cells. *Cancer Res;*66: 324-30.

10. Elger W, Schwarz S, Hedden A, Reddersen G, Schneider B (1995) Sulfamates of various estrogens are prodrugs with increased systemic and reduced hepatic estrogenicity at oral application. *J Steroid Biochem Mol Biol;*55: 395-403.

11. Leese MP, Leblond B, Smith A, Newman SP, Di Fiore A, De Simone G, et al. (2006) 2-substituted estradiol bis-sulfamates, multitargeted antitumor agents: synthesis, in vitro SAR, protein crystallography, and in vivo activity. *J Med Chem;*49: 7683-96.

12. Ho YT, Purohit A, Vicker N, Newman SP, Robinson JJ, Leese MP, et al. (2003) Inhibition of carbonic anhydrase II by steroidal and non-steroidal sulphamates. *Biochem Biophys Res Commun;*305: 909-14.

13. Supuran CT, Scozzafava A (2007) Carbonic anhydrases as targets for medicinal chemistry. *Bioorg Med Chem;*15: 4336-50.

14. Stubbs M, McSheehy PM, Griffiths JR, Bashford CL (2000) Causes and consequences of tumour acidity and implications for treatment. *Mol Med Today;*6: 15-9.

15. Pastorekova S, Ratcliffe PJ, Pastorek J (2008) Molecular mechanisms of carbonic anhydrase IX-mediated pH regulation under hypoxia. *BJU Int;*101 Suppl 4: 8-15.

16. Svastova E, Hulikova A, Rafajova M, Zat'ovicova M, Gibadulinova A, Casini A, et al. (2004) Hypoxia activates the capacity of tumor-associated carbonic anhydrase IX to acidify extracellular pH. *FEBS Lett;*577: 439-45.

17. Pettersen EF, Goddard TD, Huang CC, Couch GS, Greenblatt DM, Meng EC, et al. (2004) UCSF Chimera--a visualization system for exploratory research and analysis. *J Comput Chem;*25: 1605-12.

18. Word JM, Lovell SC, Richardson JS, Richardson DC (1999) Asparagine and glutamine: using hydrogen atom contacts in the choice of side-chain amide orientation. *J Mol Biol;*285: 1735-47.

19. Pedretti A, Villa L, Vistoli G (2004) VEGA--an open platform to develop chemo-bio-informatics applications, using plug-in architecture and script programming. *J Comput Aided Mol Des;*18: 167-73.

20. Morris GM, Huey R, Lindstrom W, Sanner MF, Belew RK, Goodsell DS, et al. (2009) AutoDock4 and AutoDockTools4: Automated docking with selective receptor flexibility. *J Comput Chem;*30: 2785-91.

21. Inc. ACD. (2006) ACD/ChemSketch Freeware. *ACD/ChemSketch Freeware*. Toronto, ON, Canada: www.acdlabs.com.

22. Krishnamurthy VM, Kaufman GK, Urbach AR, Gitlin I, Gudiksen KL, Weibel DB, et al. (2008) Carbonic anhydrase as a model for biophysical and physical-organic studies of proteins and protein-ligand binding. *Chem Rev;*108: 946-1051.

23. Tuccinardi T, Nuti E, Ortore G, Supuran CT, Rossello A, Martinelli A (2007) Analysis of human carbonic anhydrase II: docking reliability and receptor-based 3D-QSAR study. *J Chem Inf Model;*47: 515-25.

24. Totrov M, Abagyan R (2008) Flexible ligand docking to multiple receptor conformations: a practical alternative. *Curr Opin Struct Biol;*18: 178-84.

25. Genis C, Sippel KH, Case N, Cao W, Avvaru BS, Tartaglia LJ, et al. (2009) Design of a Carbonic Anhydrase IX Active-Site Mimic To Screen Inhibitors for Possible Anticancer Properties (dagger) (double dagger). *Biochemistry;*

26. Wang J, Wang W, Kollman PA, Case DA (2006) Automatic atom type and bond type perception in molecular mechanical calculations. *J Mol Graph Model;*25: 247-60.

27. Yang L, Tan CH, Hsieh MJ, Wang J, Duan Y, Cieplak P, et al. (2006) New-generation amber united-atom force field. *J Phys Chem B;*110: 13166-76.

28. Wang J, Wolf RM, Caldwell JW, Kollman PA, Case DA (2004) Development and testing of a general amber force field. *J Comput Chem;*25: 1157-74.

29. Cushman M, He HM, Katzenellenbogen JA, Lin CM, Hamel E (1995) Synthesis, antitubulin and antimitotic activity, and cytotoxicity of analogs of 2-methoxyestradiol, an endogenous mammalian metabolite of estradiol that inhibits tubulin polymerization by binding to the colchicine binding site. *J Med Chem;*38: 2041-9.

30. Leese MP, Newman SP, Purohit A, Reed MJ, Potter BV (2004) 2-Alkylsulfanyl estrogen derivatives: synthesis of a novel class of multi-targeted anti-tumour agents. *Bioorg Med Chem Lett;*14: 3135-8.

31. Edsall AB, Mohanakrishnan AK, Yang D, Fanwick PE, Hamel E, Hanson AD, et al. (2004) Effects of altering the electronics of 2-methoxyestradiol on cell proliferation, on cytotoxicity in human cancer cell cultures, and on tubulin polymerization. *J Med Chem;*47: 5126-39.

32. Tinley TL, Leal RM, Randall-Hlubek DA, Cessac JW, Wilkens LR, Rao PN, et al. (2003) Novel 2-methoxyestradiol analogues with antitumor activity. *Cancer Res;*63: 1538-49.

33. LaVallee TM, Burke PA, Swartz GM, Hamel E, Agoston GE, Shah J, et al. (2008) Significant antitumor activity in vivo following treatment with the microtubule agent ENMD-1198. *Mol Cancer Ther;*7: 1472-82.

34. Zhou Q, Gustafson D, Nallapareddy S, Diab S, Leong S, Lewis K, et al. (2010) A phase I dose-escalation, safety and pharmacokinetic study of the 2-methoxyestradiol analog ENMD-1198 administered orally to patients with advanced cancer. *Invest New Drugs;*In Print:

35. Utsumi T, Leese MP, Chander SK, Gaukroger K, Purohit A, Newman SP, et al. (2005) The effects of 2-methoxyoestrogen sulphamates on the in vitro and in vivo proliferation of breast cancer cells. *J Steroid Biochem Mol Biol;*94: 219-27.

36. Appel R, Berger G (1958) Hydrazinsulfonsäure-amide, I. Über das Hydrazodisulfamid. *Chem Berichte;*91: 1339-41.

37. Gillies RJ, Didier N, Denton M (1986) Determination of cell number in monolayer cultures. *Anal Biochem;*159: 109-13.

38. Kueng W, Silber E, Eppenberger U (1989) Quantification of cells cultured on 96-well plates. *Anal Biochem;*182: 16-9.

39. Grever MR, Schepartz SA, Chabner BA (1992) The National Cancer Institute: cancer drug discovery and development program. *Semin Oncol;*19: 622-38.

40. Berry JM, Huebner E, Butler M (1996) The crystal violet nuclei staining technique leads to anomalous results in monitoring mammalian cell cultures. *Cytotechnology;*21: 73-80.

Figure legends

Figure 1: Synthesis scheme of 2-ethyl estrone derivatives (Supporting Information S3).

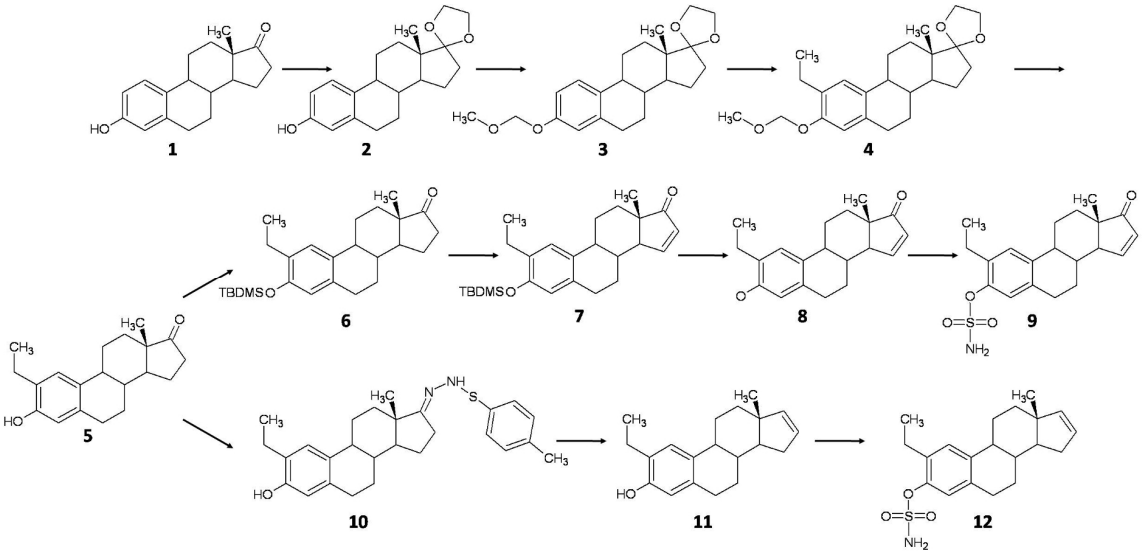

Figure 2: Correlation between Autodock free binding energy ($AD4_{\epsilon}$) and experimentally determined inhibition constant ($expK_i$). A coefficient of determination (R^2) of 0.5856 between $expK_i$ and $AD4_{\epsilon}$ was observed for docked ligands with known structures and $expK_i$.

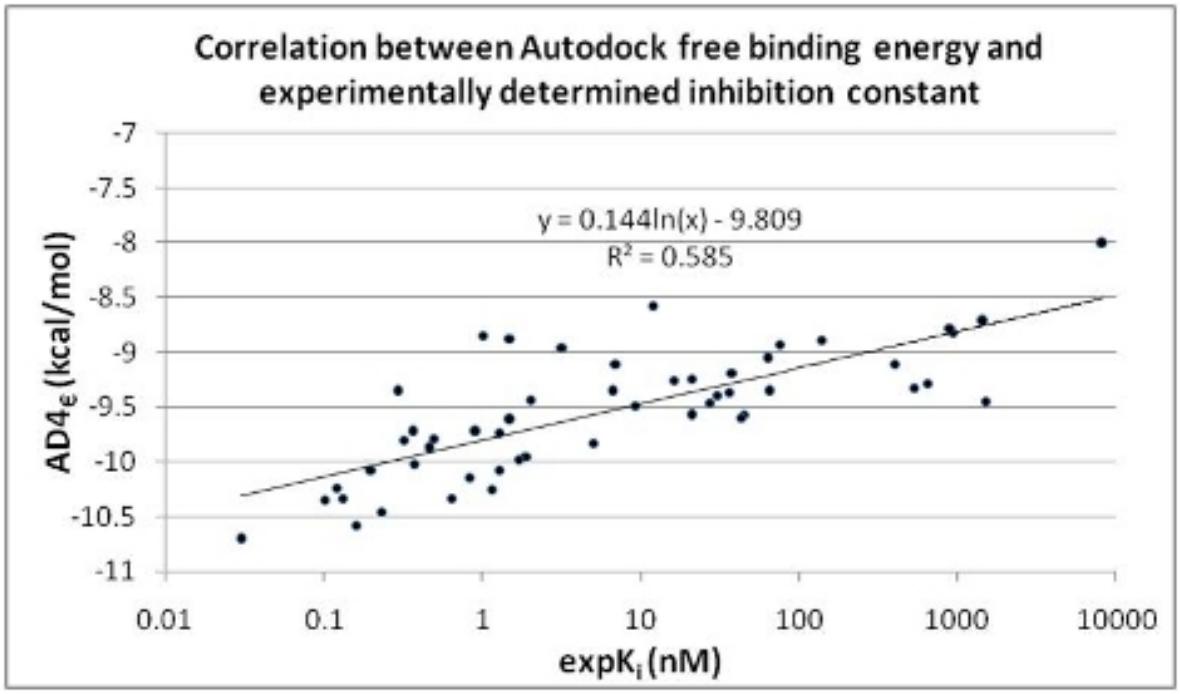

Figure 3: Docking of compound **12** in the colchicine binding site of tubulin. Hydrophobic interactions between **12** and ala250.B, leu242.B, leu248.B, leu252.B, leu255.B, lys352.B, and val318.B. Possible hydrogen bonds may also form between the sulfonamido nitrogen of the compound and tyr202.B or the val238.B oxygen.

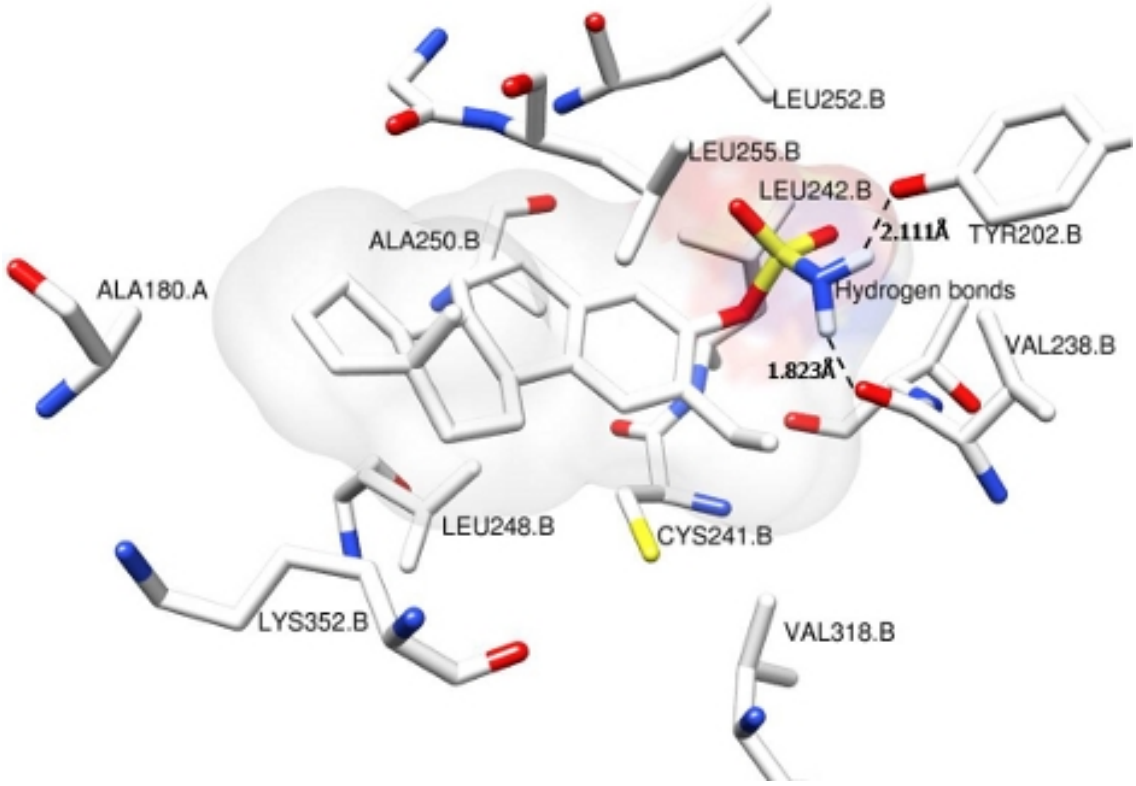

Figure 4: Vehicle-treated MDA-MB-231 control cells stained with DAPI and Alexa-488 anti-tubulin after 24 h exposure. The nucleus (A and C) of a cell undergoing normal transition from metaphase to anaphase metaphase as well as mitotic spindles and the mictotubule organizing center are observed (B and C).

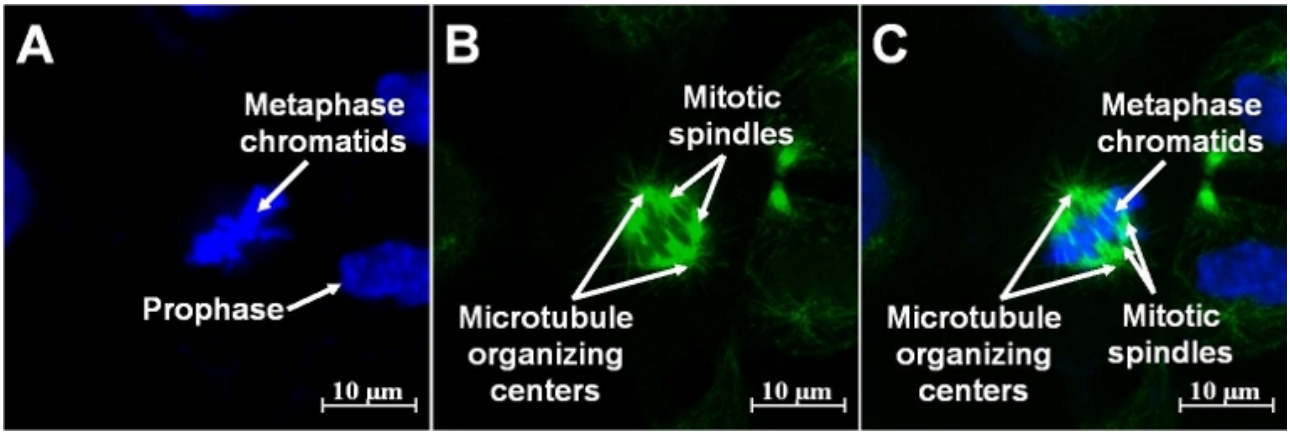

Figure 5: MDA-MB-231 cells after 24 h exposure to compound **9** and stained with DAPI and Alexa-488 anti-tubulin**.** Metaphase chromatids (A and C) and an abnormal mitotic spindle (B) are observed in compound **9**-treated cells (C).

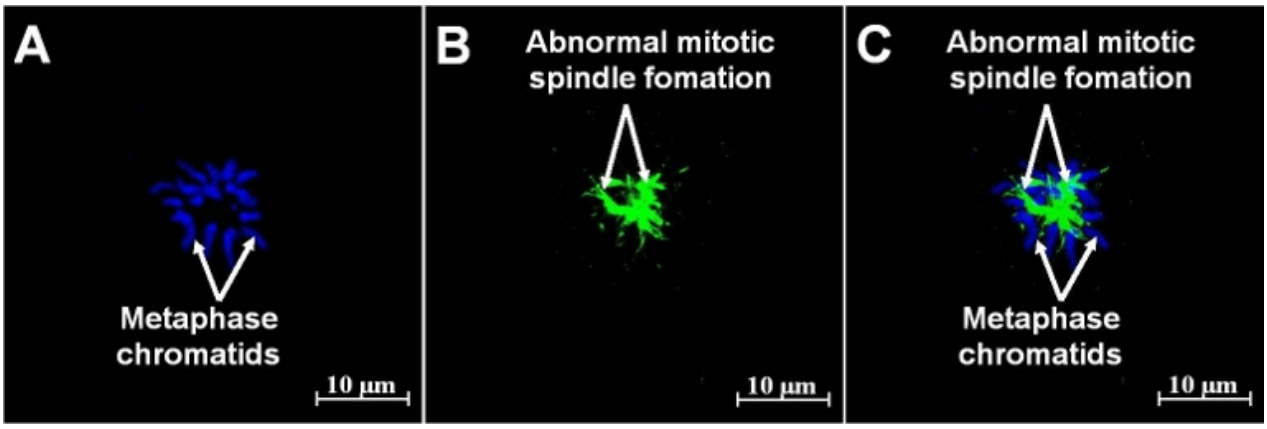

Figure 6: MDA-MB-231 cells after 24 h exposure to compound **12** and stained with DAPI and Alexa-488 anti-tubulin**.** Metaphase chromatids (A and C) and an abnormal mitotic spindle (B) are observed in compound **12** -treated cells (C).

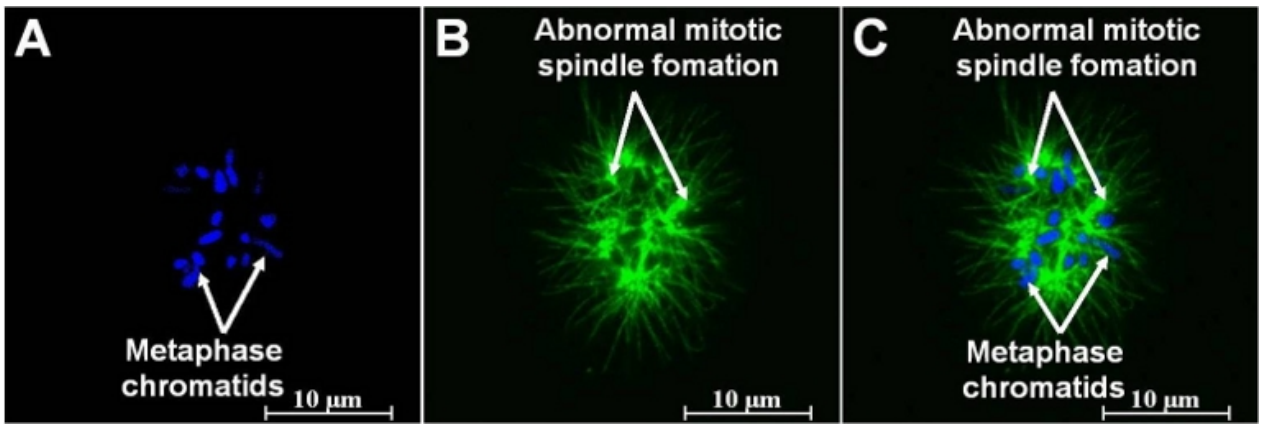

Figure 7: Measurement of DNA content of vehicle-treated, 140 nM compound **9**-treated and 200 nM compound **12**-treated MDA-MB-231 cells after 24 h of exposure as an indication of cells in various stages of cell the cell cycle. An increase in the G_2/M fraction was observed in compound **9**- and compound **12**-treated cells when compared to vehicle-treated cells. Also, an increase in the sub-G_1 fraction was observed in compound **9**- and compound **12**-treated cells.

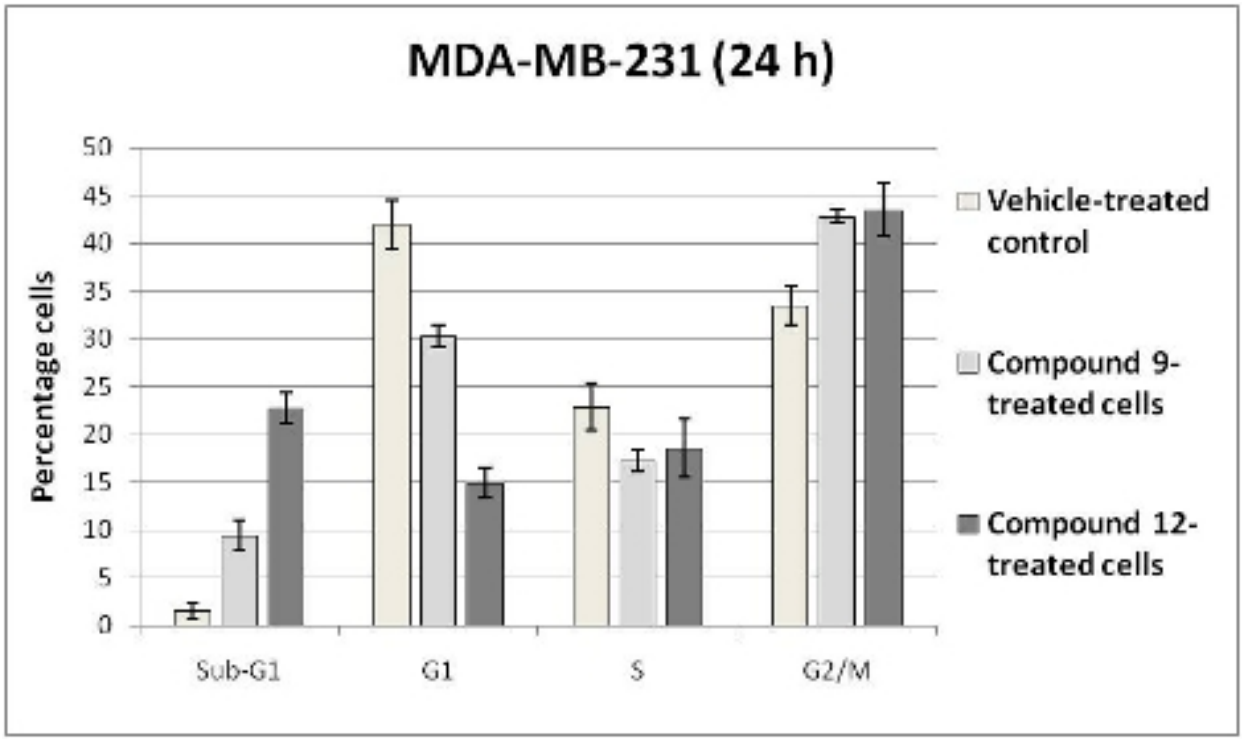

Figure 8: Measurement of DNA content of vehicle-treated, 140 nM compound **9**-treated and 200 nM compound **12**-treated MDA-MB-231 cells after 48 h of exposure as an indication of cells in various stages of cell the cell cycle. A marked increase in the sub-G_1 fraction was observed in compound **9**- and compound **12**-treated cells, indicating the induction of apoptosis after the mitotic arrest after 24 h.

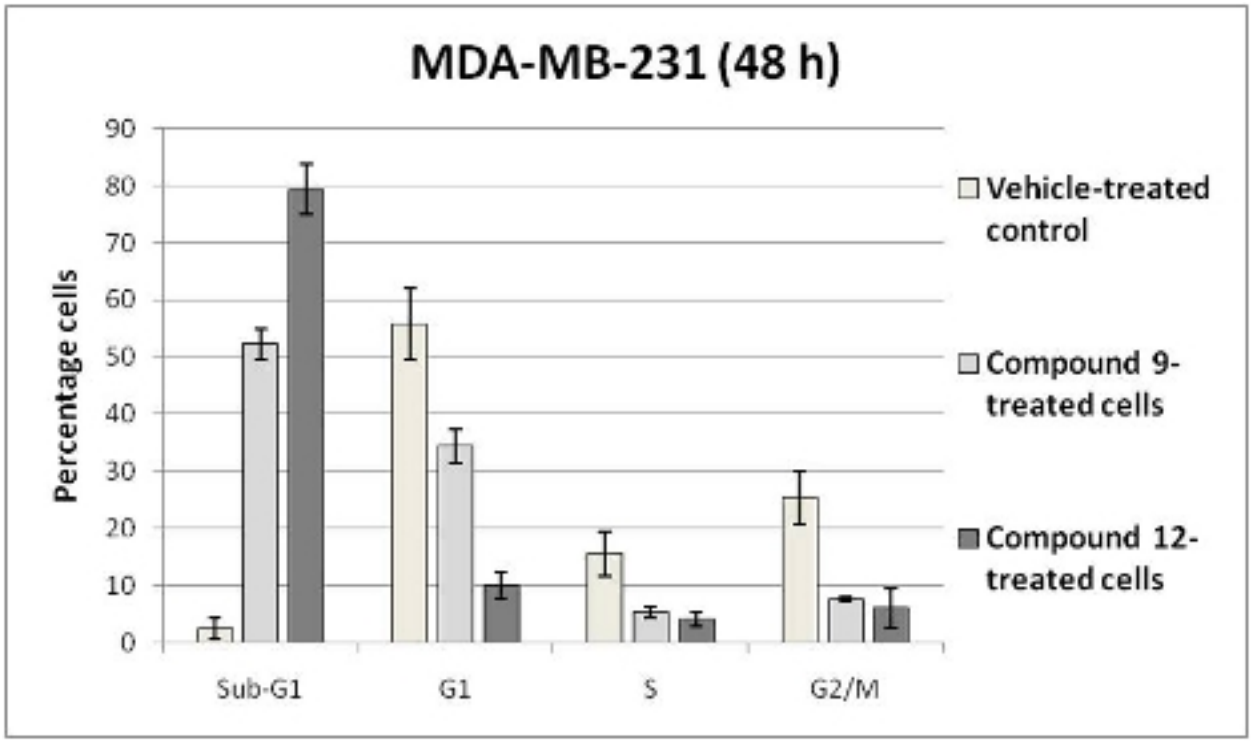

Table legends

Table 1: Growth inhibitory effect of compounds 9, 12 on MCF-7, SNO, MDA-MB-231 and HeLa. Growth inhibition = 100 x $(T-T_0)/(C-T_0)$.

50% Growth Inhibitory (GI_{50}) concentration (48h)	Compound 9 (nM)	Compound 13 (nM)
MDA-MB-231	140	200
MCF-7	130	180
SNO	110	200
HeLa	160	220

Supporting Information

	RCSB PDB accession
1	1A42
2	1BN1
3	1BN3
4	1BN4
5	1BNM
6	1BNN
7	1BNQ
8	1BNT
9	1BNU
10	1BNV
11	1BNW
12	1CIL
13	1CIM
14	1CIN
15	1EOU
16	1EOU
17	1G1D
18	1G52
19	1G53
20	1G54
21	1I8Z
22	1I90
23	1I91
24	1IF7
25	1IF8
26	1KWQ
27	1KWR
28	1OKL
29	1OKM
30	1OQ5
31	1TTM
32	1XPZ
33	1XQ0
34	1Z9Y
35	1ZE8
36	2AW1
37	2F14
38	2GD8
39	2H15
40	2HD6
41	2HL4
42	2NN1
43	2NNG
44	2NNS

45	2POU
46	2POV
47	2POW
48	3BET
49	3D8W
50	3D9Z
51	3DAZ
52	3DD0

Supporting Information S1: List of CAII structures used to generated a library of ligands to be redocked into 1OKN, 1KWR, 1CIM, 1BNW, 1CNX, 1OQ5 and 1TTM X-ray structures.

Supporting Information S10: Stacked three-dimensional image of an MDA-MB-231 cell during metaphase treated with compound **9** after 24 h.

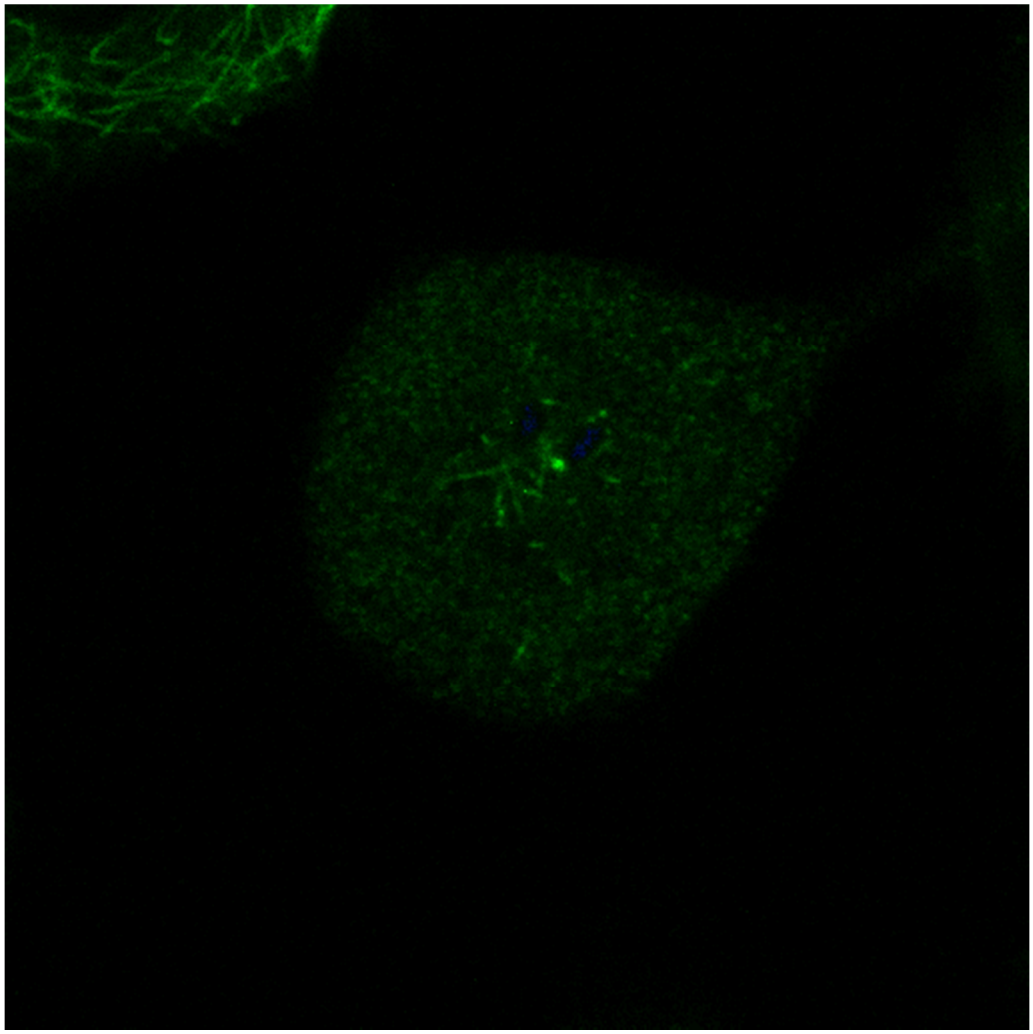

Supporting Information S11: Stacked three-dimensional image of an MDA-MB-231 cell during metaphase treated with compound **12** after 24 h.

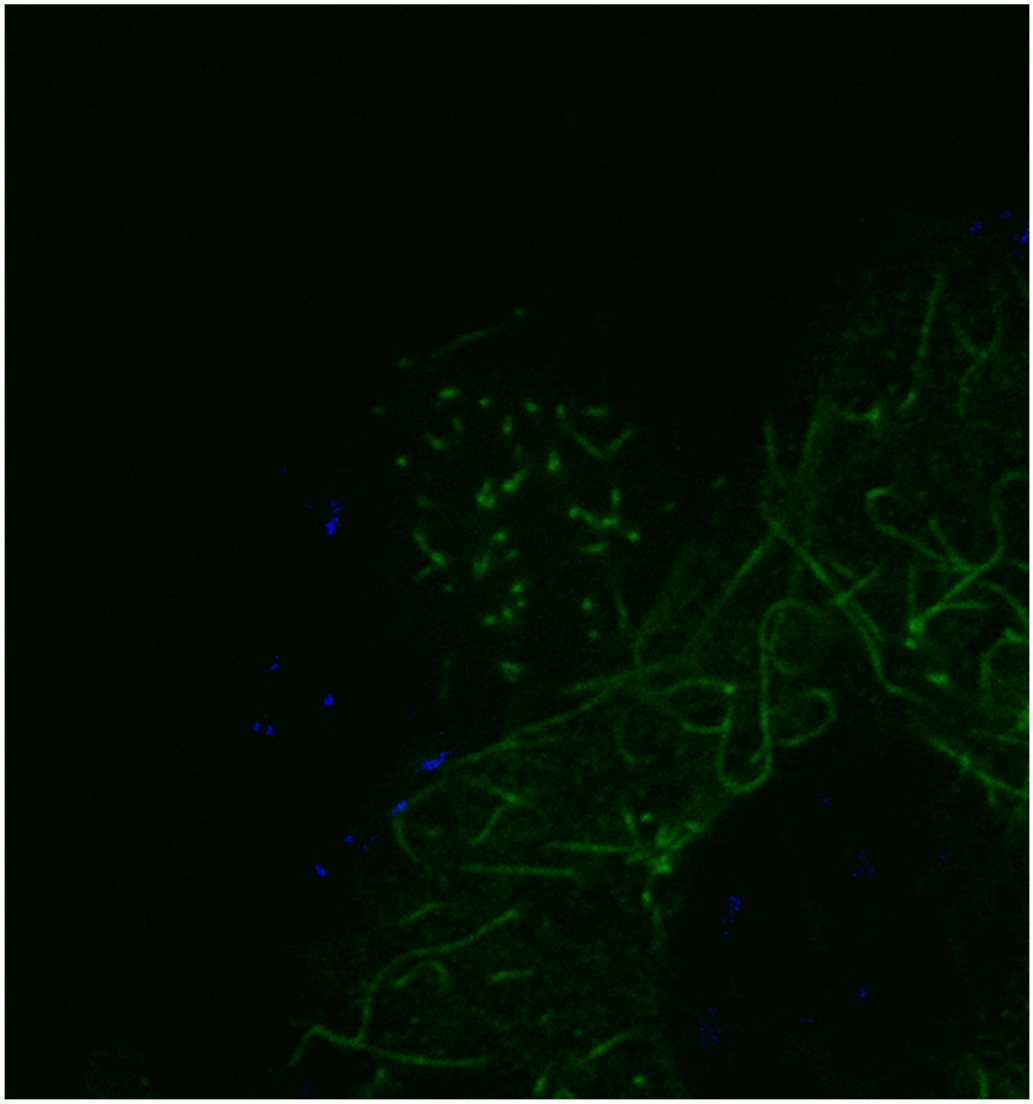

Supporting Information S2: Structures of estradiol ligands generated by modifying various constituents at position 2' and the D-ring of estrone.

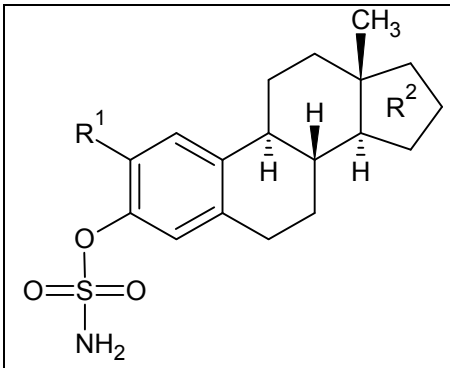		I	II	III	IV	V
		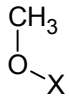	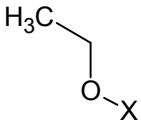	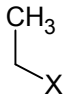	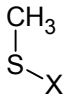	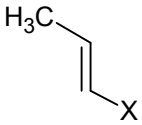
A	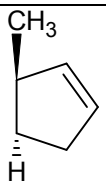	**Test 1**	**Test 18**	**Test 35**	**Test 52**	**Test 69**
B	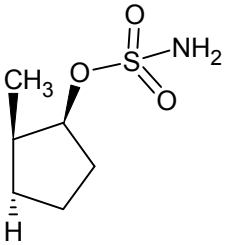	**Test 2**	**Test 19**	**Test 36**	**Test 53**	**Test 70**
C	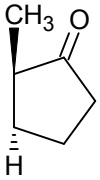	**Test 3**	**Test 20**	**Test 37**	**Test 54**	**Test 71**
D	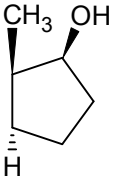	**Test 4**	**Test 21**	**Test 38**	**Test 55**	**Test 72**
E	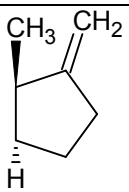	**Test 5**	**Test 22**	**Test 39**	**Test 56**	**Test 73**

F	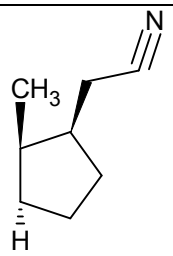	**Test 6**	**Test 23**	**Test 40**	**Test 57**	**Test 74**
G	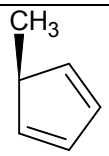	**Test 7**	**Test 24**	**Test 41**	**Test 58**	**Test 75**
H	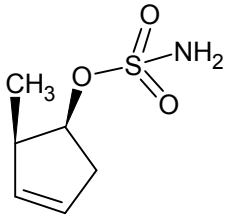	**Test 8**	**Test 25**	**Test 42**	**Test 59**	**Test 76**
I	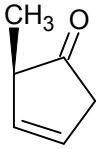	**Test 9**	**Test 26**	**Test 43**	**Test 60**	**Test 77**
J	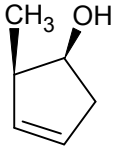	**Test 10**	**Test 27**	**Test 44**	**Test 61**	**Test 78**
K	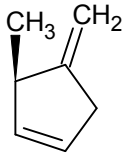	**Test 11**	**Test 29**	**Test 45**	**Test 62**	**Test 79**
L	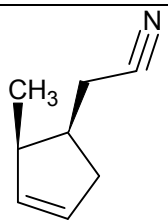	**Test 12**	**Test 30**	**Test 46**	**Test 63**	**Test 80**
M	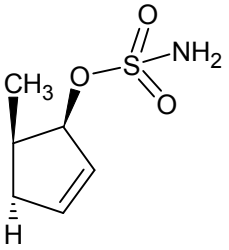	**Test 13**	**Test 31**	**Test 47**	**Test 64**	**Test 81**

N	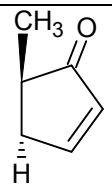	**Test 14**	**Test 32**	**Test 48**	**Test 65**	**Test 82**
O	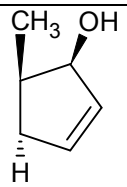	**Test 15**	**Test 33**	**Test 49**	**Test 66**	**Test 83**
P	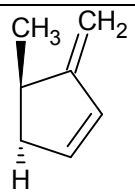	**Test 16**	**Test 34**	**Test 50**	**Test 67**	**Test 84**
Q	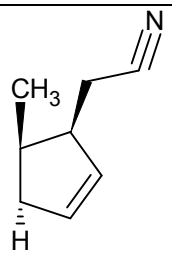	**Test 17**	**Test 36**	**Test 51**	**Test 68**	**Test 85**

Supporting Information S3: Chemistry and synthesis of estrone analogs.

Materials and methods. Chemistry. All chemicals were purchased from Aldrich Chemical Co. Organic solvents of A.R. grade were used as supplied. Anhydrous *N,N*-dimethylformamide and *N,N*-dimethylacetamide were purchased from Aldrich and stored under a positive pressure of N_2 after use. Tetrahydrofuran was distilled from sodium. Sulfamoyl chloride was prepared by an adaptation of the method of Appel and Berger (1958) and stored in a tightly sealed container in the fridge (1). Chromatography was performed on silica gel (70–230 mesh, Macherey Nagel). Thin layer chromatography was performed on Alugram® SIL G/UV_{254} aluminium backed plates (Macherey Nagel). Products were visualized with basic potassium permanganate solution. ^{1}H NMR spectra were recorded in deuterated chloroform solution (unless otherwise indicated) with a Varian 400 NMR spectrometer at 400 MHz. Chemical shifts are reported in parts per million (ppm, δ) relative to tetramethylsilane (TMS) as an internal standard.

17,17-Ethylenedioxy (2):

17,17-Ethylenedioxy estrone was synthesized according to a literature procedure (2). A suspension of estrone (27.24 g, 101 mmol), toluene (300 cm^3), ethylene glycol (30.00 cm^3, 592 mmol) and *p*-toluenesulfonic acid (0.250 g, 1.45 mmol) was refluxed for 16 hours under Dean-Stark conditions. About 2.20 ml of water was collected. The purple reaction mixture was cooled to ambient temperature and poured onto a saturated solution of sodium hydrogen carbonate (300 cm^3) and diluted with ethyl acetate (500 cm^3). The organic layer was separated and the aqueous layer was extracted with additional ethyl acetate (200 cm^3). The combined organic extract was washed with water (400 cm^3) and brine (400 cm^3). The yellow organic extract was dried over sodium sulfate, filtered and evaporated to give crude 17,17-ethylenedioxy estrone (31.5 g, 100 mmol, 99% yield) as an off-white solid which was used without further purification. An analytical sample was prepared by recrystallization from methanol: ^{1}H NMR (400 MHz, *CDCl₃*) δ 7.14 (d, *J* = 8.4 Hz, 1H), 6.61 (dd, *J* = 2.7, 8.4 Hz, 1H), 6.55 (d, *J* = 2.7 Hz, 1H), 5.10 (s, 1H), 4.00-3.84 (m, 4H), 2.91-2.70 (m, 2H), 2.40-1.20 (m, 13H), 0.88 (s, 1H). The NMR data matched those in the literature.[2]

3-O-Methoxymethyl-17,17-ethylenedioxyestrone (3):

3-O-Methoxymethyl-17,17-ethylenedioxyestrone was synthesized according to a literature procedure (2). Sodium hydride (60% dispersion in oil, 5.72 g, 143 mmol) was added in a portionwise manner to a stirred 0 °C solution of 17,17-Ethylenedioxy estrone (30.0 g, 95 mmol) in anhydrous *N,N*-dimethylformamide (420 cm^3). The cooling bath was removed and stirring was continued at ambient temperature until the evolution of hydrogen had ceased. This took about 4 hours. The orange reaction mixture was recooled to 0 °C and methyl chloromethyl ether (14.50 cm^3, 191 mmol) was cautiously added dropwise. Upon complete addition, the cooling bath was removed and the milky reaction mixture was allowed to stir at ambient temperature for 16 hours. Ammonia (2 M, 180 cm^3) was cautiously added to destroy excess methyl chloromethyl ether and sodium hydride. The aqueous reaction mixture was extracted once with ethyl acetate (850 cm^3) and the organic extract was washed with brine (5 x 300 cm^3). The organic extract was dried over sodium sulfate, filtered and evaporated to give an oil. Column chromatography (10% ethyl acetate/hexane) afforded 3-O-methoxymethyl-17,17-ethylenedioxyestrone (28.12 g, 78 mmol, 82% yield) as a viscous colourless oil that solidified on standing: R_f 0.54 (9:1 hexane/ethyl acetate). ^{1}H NMR (400 MHz, *CDCl₃*) δ 7.20 (d, *J* = 8.5 Hz, 1H), 6.82 (dd, *J* = 2.7, 8.5 Hz, 1H), 6.76 (d, *J* = 2.7 Hz, 1H), 5.13 (s, 1H), 4.02-3.84 (m, 4H), 3.47 (s, 3H), 2.90-2.77 (m, 2H), 2.40-2.17 (m, 2H), 2.10-1.20 (m, 11H), 0.88 (s, 3H). The NMR data matched those in the literature.[2]

2-Ethyl-3-O-methoxymethyl-17,17-ethylenedioxyestrone (4):

2-Ethyl-3-O-methoxymethyl-17,17-ethylenedioxyestrone was synthesized according to a modified literature procedure (2). A well stirred solution of tetramethylethylenediamine (20.00 cm^3, 133 mmol) in dry tetrahydrofuran (210 cm^3) was cooled to –78 °C and then treated with *n*-butyllithium (1.6 M, 80.00 cm^3, 128 mmol) over 10 minutes. The reaction mixture was stirred at that temperature for an additional 15 minutes. 3-O-Methoxymethyl-17,17-ethylenedioxyestrone (15.01 g, 41.9 mmol) in dry tetrahydrofuran (210 cm^3) was added by way of canula over 10 minutes. The reaction mixture was allowed to gradually warm to 0 °C. This took about 6 hours. The reaction mixture was maintained at this temperature for an additional 30 minutes and then allowed to stir at ambient temperature for 15 minutes. The reaction mixture was re-cooled to –78 °C and iodoethane (10 cm^3, 124 mmol) was added over 5 minutes. The reaction mixture was allowed to warm to ambient temperature over 2 hours and then carefully quenched with a saturated solution of aqueous ammonium chloride (50 cm^3). The aqueous reaction mixture was diluted with ethyl acetate (1000 cm^3) and water (50 cm^3) and the organic phase was separated. The organic extract was washed with an aqueous solution of sodium thiosulphite (10% m/v, 200 cm^3), more water (2 x 100 cm^3) and finally with brine (100 cm^3). The organic extract was dried over sodium sulfate, filtered and evaporated to give a pale yellow oil (17.02 g). Two column chromatographic (2.5% ethyl acetate/hexane) purifications afforded 2-ethyl-3-O-methoxymethyl-17,17-ethylenedioxyestrone (7.00 g, 18.1 mmol, 43% yield) as a viscous colourless oil. An analytical sample was recrystallized from methanol: R_f 0.10 (97.5:2.5 hexane/ethyl acetate). ^{1}H NMR (400 MHz, $CDCl_3$) δ 7.08 (s, 1H), 6.78 (s, 1H), 5.16 (s, 2H), 4.02-3.82 (m, 4H), 3.48 (s, 3H), 2.92-2.73 (m, 2H), 2.62 (q, J = 7.4 Hz, 2H), 2.41-2.16 (m, 2H), 2.10-1.95 (m, 1H), 1.94-1.70 (m, 4H), 1.70-1.28 (m, 6H), 1.19 (t, J = 7.5 Hz, 3H), 0.88 (s, 3H). The NMR data matched those in the literature.[2] Further elution of the column afforded starting material (8.00 g, 22.3 mmol, 53% recovery).

2-Ethylestrone (5):

2-Ethylestrone was synthesized according to a literature procedure (2). Methanol (68 cm^3) was cooled to 0 °C and cautiously treated with acetyl chloride (24 cm^3) and stirred for 10 minutes under nitrogen. The methanolic HCl solution was then added to a slurry of 2-Ethyl-3-O-methoxymethyl-17,17-ethylenedioxyestrone (5.000 g, 12.94 mmol) in methanol (32 cm^3) and stirred for 1 hour until all the solids had dissolved. Water (100 cm^3) was added slowly, and the reaction mixture was cooled in an ice-bath causing precipitation of the product as a white powder which was collected by filtration and washed with water (2 x 50 cm^3). The solid was air-dried under suction for 2 hours before being further dried under high-vacuum for 1 hour to afford 2-ethylestrone (3.750 g, 12.57 mmol, 97% yield) as a fluffy white solid. An analytical sample was recrystallized from methanol: R_f 0.55 (1:2 hexane/ethyl acetate). ^{1}H NMR (400 MHz, $CDCl_3$) δ 7.05 (s, 1H), 6.52 (s, 1H), 4.63 (s, 1H), 2.88-2.79 (m, 2H), 2.60 (q, J = 7.6 Hz, 2H), 2.56-2.37 (m, 2H), 2.29-1.91 (m, 5H), 1.72-1.34 (m, 6H), 1.22 (t, J = 7.6 Hz, 3H), 0.91 (s, 3H). The NMR data matched those in the literature.[2]

2-Ethyl-(tert-butyldimethylsilyl)estrone (6):

N,N-Dimethylformamide (25 cm^3) was added to a dry round bottom flask and the solvent was stirred under nitrogen. 2-Ethylestrone (2.000 g, 6.70 mmol), imidazole (1.250 g, 18.36 mmol), and *tert*-butyldimethylsilyl chloride (1.470 g, 9.75 mmol) were added sequentially and stirring was continued for 20 hours. The solvent was evaporated to give a brown oil. Column chromatography (5% ethyl acetate/hexane) afforded 2-ethyl-(tert-butyldimethylsilyl)estrone (2.595 g, 6.29 mmol, 94% yield) as a white solid: R_f 0.20 (19:1 hexane/ethyl acetate). ^{1}H NMR (400 MHz, $CDCl_3$) δ 7.05 (s, 1H), 6.49 (s, 1H), 2.92-2.74 (m, 2H), 2.56 (q, J = 7.5 Hz, 2H), 2.53-2.38 (m, 2H), 2.32-1.89 (m, 5H), 1.72-1.34 (m, 6H), 1.16 (t, J = 7.5 Hz, 3H), 1.01 (s, 9H), 0.91 (s, 3H), 0.23 (s, 6H).

2-Ethyl-(tert-butyldimethylsilyl)estra-1,3,5(10),15-tetraen-3-ol-17-one (7):

2-Ethyl-(tert-butyldimethylsilyl)estra-1,3,5(10),15-tetraen-3-ol-17-one was synthesized based upon a literature procedure (3). To a solution of diisopropylamine (0.50 cm^3, 2.90 mmol) in dry tetrahydrofuran (10 cm^3) at 0 °C and under a nitrogen atmosphere was added a solution of *n*-butyllithium (1.6 M, 2.20 cm^3, 2.91 mmol). Stirring was continued at 0 °C for 15 minutes before cooling to –78 °C. A solution of 2-ethyl-3-O-methoxymethyl-17,17-ethylenedioxyestrone (0.500 g, 1.21 mmol) in tetrahydrofuran (10 cm^3) was added dropwise over 5 minutes after which the mixture was stirred for an additional 40 minutes. Trimethylsilyl chloride (0.40 cm^3, 2.58 mmol) was injected via syringe and then the reaction mixture was allowed to warm to ambient temperature. Water (10 cm^3) was added and the reaction mixture was extracted into diethyl ether-dichloromethane (3:2, 3 x 20 cm^3) and washed once with brine (20 cm^3). The combined organic extracts were dried over sodium sulfate, filtered and evaporated to give a viscous yellow oil. The residue was dissolved into benzonitrile (20 cm^3). Palladium(II) acetate (0.272 g, 1.21 mmol) was added followed immediately by 5 cycles of degassing and purging the reaction mixture with nitrogen. The reaction mixture was stirred for 20 hours at ambient temperature. The solvent was evaporated to give a black oil. Column chromatography (5% ethyl acetate/hexane) afforded starting material (0.050 g, 10% recovery) followed by 2-ethyl-(tert-butyldimethylsilyl)estra-1,3,5(10),15-tetraen-3-ol-17-one (0.300 g, 0.73 mmol, 60% yield) as a white solid: R_f 0.10 (19:1 hexane/ethyl acetate). ^{1}H NMR (400 MHz, $CDCl_3$) δ 7.67-7.58 (m, 1H), 7.10-7.01 (m, 1H), 6.54-6.48 (m, 1H), 6.08 (dd, J = 3.2, 6.0 Hz, 1H), 2.96-2.80 (m, 2H), 2.57 (q, J = 7.5 Hz, 2H), 2.54-2.42 (m, 2H), 2.40-2.27 (m, 1H), 2.23-2.12 (m, 1H), 2.07-1.96 (m, 1H), 1.88-1.64 (m, 3H), 1.61-1.47 (m, 2H), 1.17 (t, J = 7.5 Hz, 3H), 1.11 (s, 3H), 1.01 (s, 9H), 0.23 (s, 6H).

2-Ethyl-estra-1,3,5(10),15-tetraen-3-ol-17-one (8):

Dry tetrahydrofuran (100 cm^3) was added to 2-Ethyl-(tert-butyldimethylsilyl)estra-1,3,5(10),15-tetraen-3-ol-17-one (0.600 g, 1.46 mmol) and cooled to –78 °C with stirring under nitrogen. A solution of tetrabutylammonium fluoride in tetrahydrofuran (1.0 M, 2.20 cm^3) was slowly added dropwise and stirring was continued for 5 minutes. The reaction was quenched with water (20 cm^3) and diluted with ethyl acetate (200 cm^3). The water was separated and the organic extract was washed with brine (50 cm^3). The organic extract was dried over sodium sulfate, filtered and evaporated to give a yellow residue. Column chromatography (20% ethyl acetate/hexane) afforded 2-ethyl-estra-1,3,5(10),15-tetraen-3-ol-17-one (0.408 g, 1.38 mmol, 94% yield) as a white solid: R_f 0.10 (4:1 hexane/ethyl acetate). ^{1}H NMR (400 MHz, $CDCl_3$) δ 7.63 (ddd, *J* = 0.7, 1.8, 6.0 Hz, 1H), 7.05 (s, 1H), 6.54 (s, 1H), 6.09 (dd, *J = 3.2,* 6.0 Hz, 1H), 4.82 (s, 1H), 2.98-2.81 (m, 2H), 2.61 (q, *J* = 7.5 Hz, 2H), 2.55-2.41 (m, 2H), 2.39-2.27 (m, 1H), 2.22-2.11 (m, 1H), 2.08-1.98 (m, 1H), 1.89-1.46 (m, 4H), 1.23 (t, *J* = 7.5 Hz, 3H), 1.11 (s, 3H).

2-Ethyl-3-O-sulfamoyl-estra-1,3,5(10),15-tetraen-3-ol-17-one (9):

2-Ethyl-estra-1,3,5(10),15-tetraen-3-ol-17-one (0.120 g, 0.41 mmol) was added to *N,N*-dimethylacetamide (1.00 cm^3) and stirred under nitrogen at 0 °C. Sulfamoyl chloride (0.141 g, 1.22 mmol) was added and the reaction mixture was allowed to warm to ambient temperature over 16 hours. Ethyl acetate (25 cm^3) and water (25 cm^3) were added, and the organic layer was separated and washed with additional water (4 x 25 cm^3) and brine (25 cm^3). The organic extract was dried over sodium sulfate, filtered and evaporated to give a green oil. Column chromatography (40% ethyl acetate/hexane) afforded 2-ethyl-3-O-sulfamoyl-estra-1,3,5(10),15-tetraen-3-ol-17-one (0.075 g, 0.20 mmol, 49% yield) as a foam. The solid was stored in the freezer when not in use: R_f 0.42 (3:2 hexane/ethyl acetate) ^{1}H NMR (400 MHz, $CDCl_3$) δ 7.68-7.54 (m, 1H), 7.08 (s, 1H), 7.06 (s, 1H), 6.23 (dd, *J* = 2.1, 5.9 Hz, 1H), 4.99 (s, 2H), 2.95-2.81 (m, 3H), 2.67 (q, *J* = 7.6 Hz, 2H), 2.36-2.17 (m, 2H), 2.05-1.92 (m, 2H), 1.89-1.77 (m, 1H), 1.74-1.53 (m, 2H), 1.53-1.40 (m, 1H), 1.19 (t, *J* = 7.6 Hz, 3H), 1.16 (s, 3H).

2-Ethyl-estra-17-methylbenzenesulfenohydrazide (10):

2-Ethylestrone (0.515 g, 1.73 mmol) and *p*-toluenesulfonyl hydrazide (0.402 g, 2.16 mmol) in methanol (15 cm^3) were heated under reflux for 16 hours. The reaction mixture was evaporated to half its volume and allowed to crystallize. The crystalline product was decanted from the mother liquor and washed with methanol (2 x 2 cm^3). A further crop of solids were realized by slow evaporation of the mother followed by washing with methanol (3 x 2 cm^3). The combined solids were dried under high vacuum to afford 2-ethyl-estra-17-methylbenzenesulfenohydrazide (0.621 g, 1.33 mmol, 77% yield) as a pale yellow solid: R_f 0.23 (3:1 hexane/ethyl acetate). ^{1}H NMR (400 MHz, $CDCl_3$) δ 7.85 (d, J = 8.5 Hz, 2H), 7.30 (d, J = 8.5 Hz, 2H), 7.14 (s, 1H), 7.03 (br s, 1H), 6.49 (s, 1H), 4.76 (br s, 1H), 2.85-2.71 (m, 2H), 2.59 (q, J = 7.5 Hz, 2H), 2.43 (s, 3H), 2.41-2.23 (m, 2H), 2.23-2.00 (m, 3H), 1.98-1.81 (m, 2H), 1.54-1.25 (m, 6H), 1.22 (t, J = 7.5 Hz, 3H), 0.81 (s, 3H).

2-Ethyl-17estra-1,3,5(10)16-tetraene (11):

2-Ethyl-estra-17-methylbenzenesulfenohydrazide (0.300 g, 0.64 mmol) was dissolved into dry tetrahydrofuran (20 cm^3) and cooled to –10 °C under nitrogen. *n*-Butyllithium (1.6 M, 1.40 cm^3, 2.24 mmol) was added dropwise over 2 minutes. The orange reaction mixture was allowed to warm to ambient temperature and stirring was continued for 3 days. Ice (5 g) was added followed by a saturated aqueous ammonium chloride solution (5 cm^3). The organic phase was separated and the aqueous phase was washed with diethyl ether (10 cm^3). The combined organic extracts were washed with a saturated solution of sodium hydrogen carbonate (10 cm^3) followed by a single wash with brine (10 cm^3). The organic extract was dried over sodium sulfate and evaporated to give a yellow gum. Column chromatography (10% ethyl acetate/hexane) afforded 2-ethyl-17estra-1,3,5(10)16-tetraene (0.122 g, 0.43 mmol, 67% yield) as a viscous yellow oil that readily darkened on standing. The thick oil was stored in the freezer as it appeared unstable at ambient temperature: R_f 0.40 (4:1 hexane/ethyl acetate). ^{1}H NMR (400 MHz, $CDCl_3$) δ 7.04 (s, 1H), 6.50 (s, 1H), 5.91 (ddd, J = 1.1, 2.4, 5.7 Hz, 1H), 5.74 (ddd, J = 1.5, 3.0, 5.7 Hz, 1H), 4.51 (br s, 1H), 2.92-2.72 (m, 2H), 2.60 (q, J = 7.5 Hz, 2H), 2.40-2.18 (m, 3H), 2.06-1.85 (m, 3H), 1.64-1.36 (m, 5H), 1.22 (t, J = 7.5 Hz, 3H), 0.79 (s, 3H).

2-Ethyl-3-O-sulfamoyl-estra-1,3,5(10)16-tetraene (12):

Sulfamoyl chloride (0.150 g, 1.30 mmol) was added to an ice-cold solution of 2-ethyl-17estra-1,3,5(10)16-tetraene (0.105 g, 1.00 mmol) in *N,N*-dimethylacetamide (1.5 cm^3). The reaction was allowed to warm to ambient temperature overnight. Ethyl acetate (25 cm^3) and water (25 cm^3) were added, and the organic layer was separated and washed with additional water (4 x 25 cm^3) and brine (25 cm^3). The organic extract was dried over sodium sulfate, filtered and evaporated to give a green oil. Column chromatography (ethyl acetate) afforded 2-ethyl-3-O-sulfamoyl-estra-1,3,5(10)16-tetraene (0.128 g, 0.35 mmol, 95% yield) as an orange gum. The gum was stored in the freezer as it appeared unstable at ambient temperature. R_f 0.50 (ethyl acetate). ^{1}H NMR (400 MHz, $CDCl_3$) δ 7.17 (s, 1H), 7.06 (s, 1H), 5.97-5.87 (m, 1H), 5.78-5.70 (m, 1H), 5.12 (br s, 2H), 2.96-2.79 (m, 2H), 2.69 (q, J = 7.6 Hz, 2H), 2.41-2.12 (m, 3H), 2.02-1.83 (m, 3H), 1.69-1.38 (m, 5H), 1.21 (t, J = 7.6 Hz, 3H), 0.79 (s, 3H).

REFERENCES

1. Appel R, Berger G (1958) Hydrazinsulfonsäure-amide, I. Über das Hydrazodisulfamid. *Chem Berichte;***91**: 1339-41.
2. Leese MP, Hejaz HA, Mahon MF, Newman SP, Purohit A, Reed MJ, et al. (2005) A-ring-substituted estrogen-3-O-sulfamates: potent multitargeted anticancer agents. *J Med Chem;***48**: 5243-56.
3. Ito Y, Hirao T, Saegusa T (1978) Synthesis of α/β-Unsaturated Carbonyl Compounds by Palladium(II)-Catalyzed Dehydrosilylation of Silyl Enol Ethers. *J Org Chem;***43**: 1011-3.

Supporting Information S4: High resolution mass spectrometry (HR-MS) data for synthesized compounds.

Compounds	Molecular wt (Theoretical)	Molecular wt (Mass Spectrometry)	HPLC retention time in min
1	270.36608	270.16136	1.6
2	314.41864	314.18899	0.83
3	358.4712	358.21398	0.73
4	386.52436	386.24606	0.62
5	298.41924	298.19295	0.62
6	412.6801	412.27935	0.48
7	410.66422	410.25954	1.18
8	296.40336	296.1812	1.49
9	375.4818	375.15514	1.64-2.17
10	466.63546	466.23993	0.94
11	282.41984	282.19812	0.54
12	361.49828	361.16929	2.29-2.34

Supporting Information S5: Best docked energy of estrone analogs docked into the colchicine bindings sites of 1SA0, 1SA1, 1Z2B, 3DU7, and 3E22 X-ray structures.

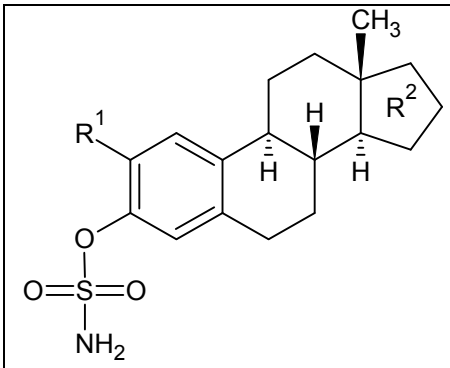			I	II	III	IV	V
			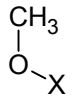	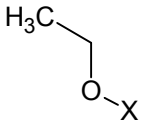	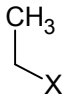	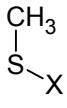	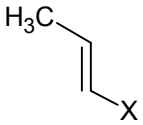
		Rank	**2**	**5**	**1**	**4**	**3**
A	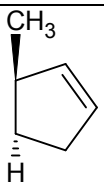	**13**	-10.05	-9.79	-10.06	-9.75	-9.48
B	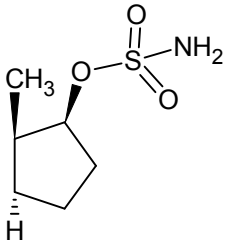	**2**	-11.04	-11.02	-11.05	-10.85	-10.99
C	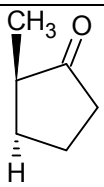	**11**	-10.21	-9.69	-10.31	-10.05	-9.9
D	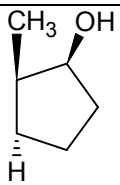	**17**	-10.02	-9.38	-10.04	-9.5	-9.75
E	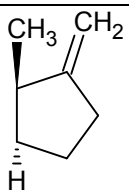	**9**	-10.39	-9.94	-10.19	-10.12	-10.06

F	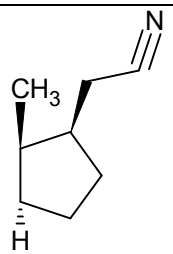	**3**	-11.34	-10.58	-11.53	-10.32	-11.01
G	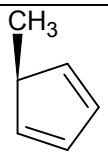	**14**	-9.58	-9.71	-9.96	-10.06	-9.96
H	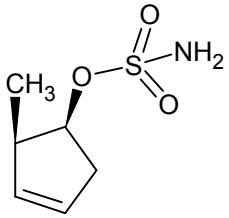	**1**	-10.83	-11.1	-11.43	-11.03	-11.27
I	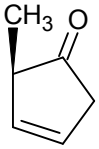	**12**	-9.71	-9.75	-10.24	-9.99	-10.32
J	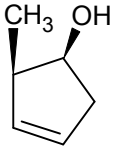	**15**	-9.73	-10.02	-9.98	-9.67	-9.74
K	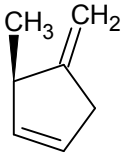	**7**	-10.2	-10.13	-10.57	-10.66	-10.61
L	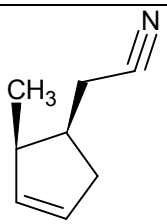	**6**	-10.68	-10.43	-11.22	-10.51	-10.88
M	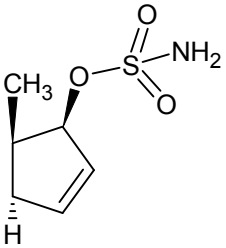	**4**	-10.8	-10.73	-10.75	-10.91	-11.06

N	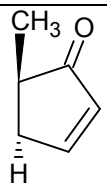	**10**	-10.19	-10.18	-10.28	-9.99	-10.04
O	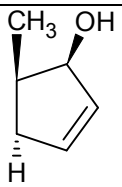	**16**	-9.88	-9.58	-10.04	-9.76	-9.79
P	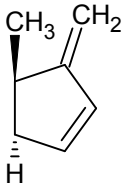	**8**	-10.24	-10.33	-10.34	-10.13	-9.91
Q	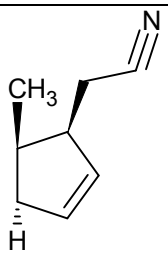	**5**	-10.95	-10.47	-11.28	-10.37	-10.62

Supporting Information S6: Best docked energy of CAII ligands docked into 1OKN, 1KWR, 1CIM, 1BNW, 1CNX, 1OQ5 and 1TTM X-ray structures.

RCSB PDB accession code	K_i	Best Autodock 4.0 docking energy	RMSD
2NNG	8200	-8.01	1.67
3BET	1500	-9.45	1.02
1OKM	1450	-8.72	2.86
1OKL	930	-8.82	0.42
2NNS	900	-8.78	2.01
2H15	640	-9.29	1.78
2GD8	526	-9.33	0.77
2NN1	400	-9.11	1.18
1XQ0	137	-8.89	2.32
2POV	75	-8.93	0.69
1Z9Y	65	-9.36	1.98
2POW	63	-9.06	2.83
1TTM	45	-9.57	1.69
2AW1	43	-9.6	2.03
2POU	38	-9.19	0.52
1EOU	36	-9.37	1.97
2HL4	30	-9.39	2.07
1XPZ	27	-9.46	2.61
1OQ5	21	-9.58	0.68
1ZE8	21	-9.24	1.34
2HD6	16	-9.26	2.64

3DAZ	11.8	-8.58	2.41
1KWQ	9.21	-9.49	1.77
3D8W	7	-9.11	0.97
1KWR	6.61	-9.36	1.89
1EOU	5	-9.83	1.99
1A42	3.2	-8.96	0.85
3D9Z	2	-9.44	1.82
1CIN	1.9	-9.95	0.81
1BNV	1.7	-9.98	0.83
1CIM	1.5	-9.62	0.67
1G54	1.5	-8.88	1.07
1I90	1.28	-9.74	3.62
1I8Z	1.27	-10.08	0.98
1I91	1.15	-10.25	2.87
3DD0	1	-8.85	1.1
1G53	0.91	-9.73	3.62
1BNW	0.83	-10.15	3.07
2F14	0.64	-10.34	3.48
1BN4	0.49	-9.79	2.74
1BN1	0.46	-9.88	2.14
1CIL	0.37	-10.02	1.25
1G1D	0.36	-9.73	3.67
1BNQ	0.32	-9.8	1.25
1G52	0.29	-9.36	1.05

1IF8	0.23	-10.46	1.94
1BNU	0.2	-10.08	1.14
1BNT	0.16	-10.58	1.51
1BN3	0.13	-10.34	0.62
1BNN	0.12	-10.24	0.48
1BNM	0.1	-10.35	0.87
1IF7	0.03	-10.71	2.64

Supporting Information S7: Best docked energy of estrone analogs docked into 1OKN, 1KWR, 1CIM, 1BNW, 1CNX, 1OQ5 and 1TTM for X-ray structures for CAII and 3DC9, 3DCS, 3DCC, 3DC3, 3DCW and 3DBU X-ray structures for CAIX.

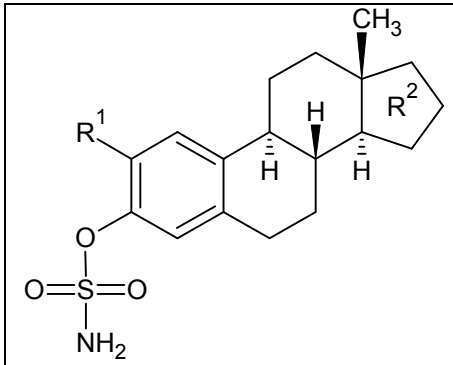		I		II		III		IV		V	
		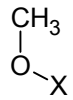		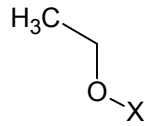		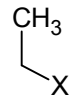		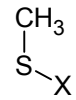		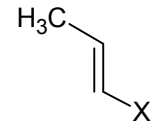	
		Autodock 4.0 docking energy after docking into CAIX and CAII									
		CAIX	CAII	CAIX	CAII	CAIX	CAII	CAIX	CAII	CAIX	CAII
A	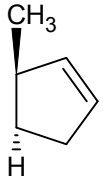	-9.86	-9.72	-9.64	-9.78	-10.06	-9.89	-9.41	-9.72	-8.41	-9.90
B	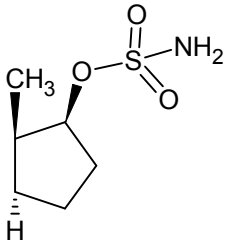	-9.13	-9.02	-9.03	-9.46	-9.14	-9.58	-9.30	-9.57	-9.43	-9.81

C	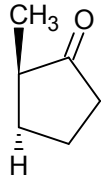	-9.70	-9.73	-9.47	-9.56	-9.90	-9.89	-9.15	-9.59	-7.96	-9.70
D	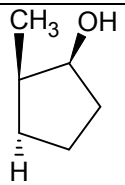	-9.46	-9.27	-8.51	-9.30	-9.32	-9.48	-9.34	-9.51	-7.69	-9.48
E	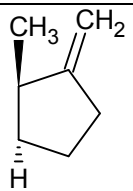	-9.66	-9.84	-9.02	-9.91	-9.78	-10.01	-9.73	-9.85	-7.94	-9.88
F	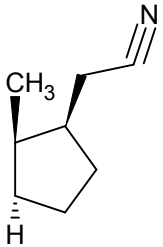	-9.04	-8.90	-8.12	-9.81	-9.07	-9.54	-8.67	-9.68	-7.90	-9.59
G	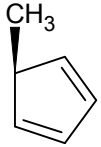	-9.49	-9.64	-9.13	-9.83	-9.80	-9.94	-9.11	-9.78	-8.14	-10.33
H	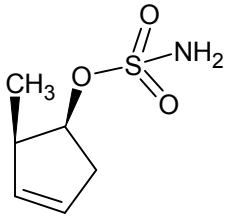	-9.46	-9.48	-9.45	-9.52	-9.44	-9.69	-9.30	-9.47	-9.78	-9.78

I	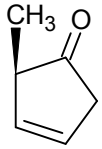	-9.50	-9.68	-8.94	-9.79	-9.77	-9.97	-9.00	-9.75	-8.14	-10.03
J	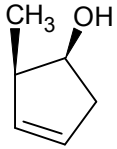	-9.32	-9.51	-8.69	-9.51	-9.45	-9.80	-8.82	-9.46	-7.83	-9.72
K	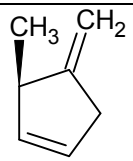	-9.82	-9.94	-8.68	-9.80	-10.07	-10.08	-9.40	-10.04	-8.40	-10.11
L	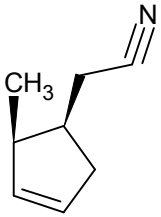	-9.70	-9.82	-8.83	-9.66	-9.55	-9.97	-9.62	-9.85	-8.11	-9.88
M	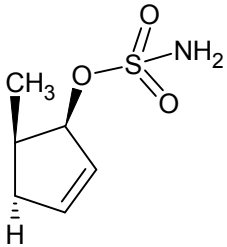	-9.23	-9.64	-9.31	-9.51	-9.28	-9.51	-9.43	-9.61	-9.22	-10.04
N	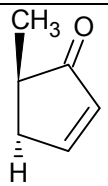	-9.77	-9.59	-9.49	-9.45	-9.88	-9.69	-8.84	-9.55	-8.26	-9.73

O	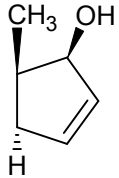	-9.20	-9.27	-8.54	-9.38	-9.24	-9.45	-8.10	-9.21	-7.73	-9.53
P	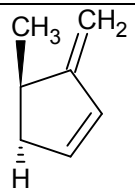	-9.90	-9.74	-9.00	-9.70	-9.96	-9.79	-9.52	-9.80	-8.32	-9.99
Q	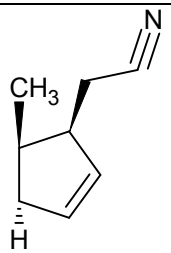	-8.98	-9.53	-8.94	-9.65	-8.88	-9.73	-8.49	-9.51	-8.14	-9.69

Supporting Information S8: Stacked three-dimensional image of a vehicle-treated MDA-MB-231 cell in prophase.

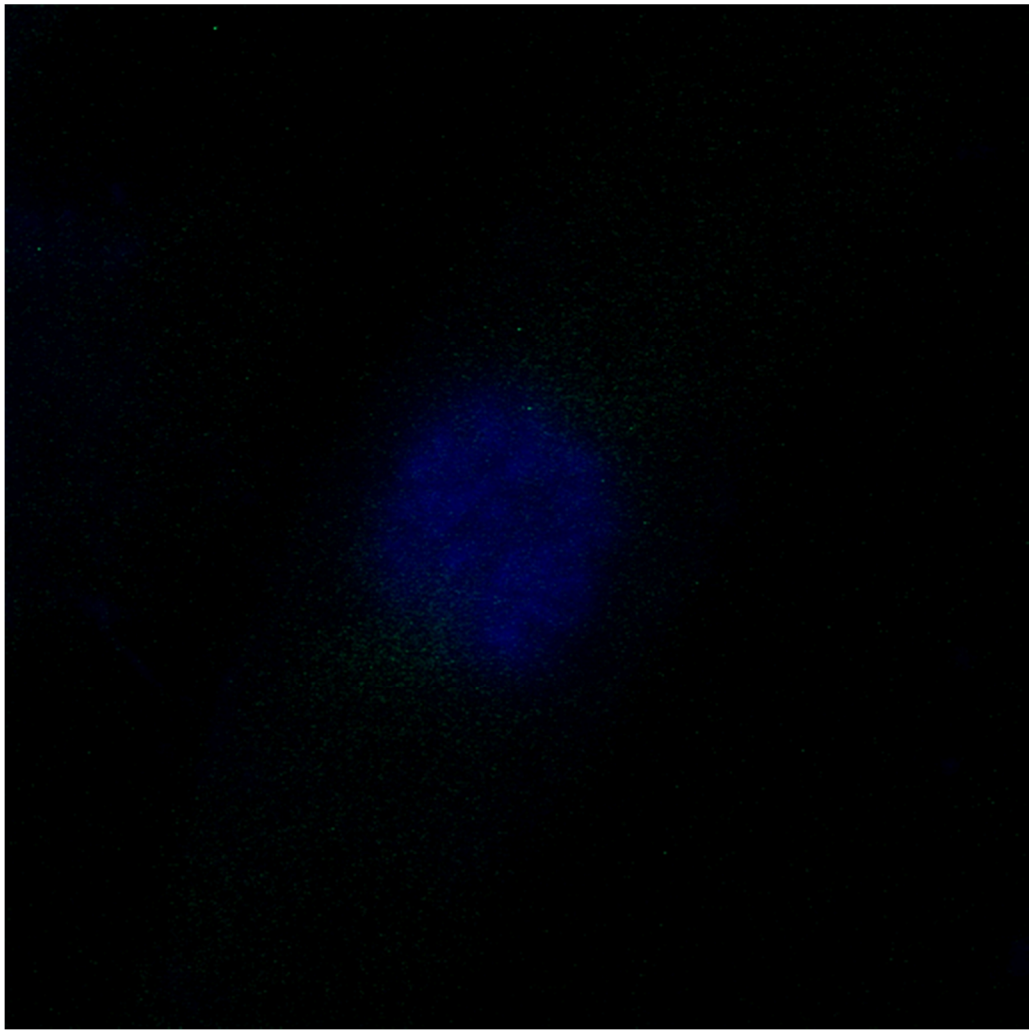

Supporting Information S9: Stacked three-dimensional image of a vehicle-treated MDA-MB-231 cell in telophase.